Local Surface Modification of Quartz Glass by the Laser-Induced Reactive Deposition of Carbon Clusters

Saho Osone[1], Makoto Hirasawa[2], Mikio Kumita[1],
Hidenori Higashi[1], Kazuya Sawada[1], Kazutaka Hara[1],
Atsushi Matsuki[1], Takafumi Seto[1], Yoshio Otani[1],
Eiji Taguchi[3] and Hidehiro Yasuda[3]

[1] *Faculty of Natural System, Kanazawa University, Kakuma-machi, Kanazawa–shi, Ishikawa 920-1192, Japan*
[2] *National Institute of Advanced Industrial Science and Technology (AIST), 1-2-1 Namiki, Tsukuba–shi, Ibaraki 305-8564, Japan*
[3] *Research Center for Ultra-High Voltage Electron Microscopy, Osaka University, Mihogaoka 7-1 Ibaraki–shi, Osaka 567-0047, Japan*

The surface of quartz glass was modified by the pulsed laser deposition of carbon clusters. A carbon target was irradiated by a pulsed laser transmitted through a quartz glass substrate to excite the carbon clusters deposited on the surface of the quartz. After continuous laser irradiation for several minutes, the resulting film on the irradiated spot (2 mm in diameter) was found to be optically transparent, but to exhibit electrical conductivity. The Raman spectrum of the irradiated region contained clear G and 2D band peaks, a likely sign of thin layers of graphite structures, but it also contained a D band peak originating from defects. The surface-modified regions were analyzed in detail using transmission electron microscopy and X-ray photoelectron spectroscopy. The analyses suggested that silicon carbide (SiC) generated by the laser-induced reaction between the carbon clusters and quartz substrate may have played an important role in the formation of the transparent conductive region on the surface of the quartz glass.

Introduction

The surface treatment of glass is a key technology for the functionalization of glass surfaces. One of the most important processes in the manufacture of optical devices is the antireflection coatings on glass surfaces (Chhajed *et al.*, 2008). Transparent conductive films (TCFs) are essential components of electro-optical devices used in photovoltaic and display applications (Bonaccorso *et al.*, 2010). Plasma treatment is also effective for modifying the physicochemical properties of glass surfaces (Krishnamurthy and Kamel, 1989).

The local (small area) surface modification of glass is an increasingly important process for the miniaturization of optical devices and electrical circuits. Possible applications for local modification include the micro-shaping, polishing, and damage repair of glass surfaces using focused laser beams (Matthews *et al.*, 2015).

Carbon is one of the most promising candidates among the various materials used for the treatment of glass surfaces. In addition to being free of rare metals and chemically stable, carbon exhibits unique properties in the low-dimensional system, i.e., nanocarbons. Graphene, a material composed of crystalline monolayers of sp²-hybridized carbon, is considered a candidate material for the next generation of TCFs (Geim and Novoselov, 2007; Geim, 2009). A unique electron transport phenomenon observed on the two-dimensional atomic monolayers of graphene allows for extremely high charge mobility and the transmission of visible light. As a consequence, graphene is considered a possible substitute for indium tin oxide which is currently used as TCFs (Granqvist and Hultaker, 2002).

Tremendous efforts have been made to find optimum routes to the synthesis of high-quality graphene on an industrial scale (Zheng *et al.*, 2010). The routes so far investigated have included mechanical exfoliation of highly ordered pyrolytic graphite (HOPG) (Qian *et al.*, 2011), chemical vapor deposition (CVD) on catalytic layers (Wei *et al.*, 2013), and pulsed laser deposition (PLD) (Wang *et al.*, 2011). Yet, most of these processes require the subsequent transfer of the graphene to the surface of a transparent substrate (Li *et al.*, 2009) such as a glass or polymer, which significantly reduces the production yield and increases the risk of contamination.

The direct synthesis of a transparent and conductive layer on the specific area of a glass surface offers the advantages of a reduced production cost and higher yield. Wei *et al.* (2013) recently reported a method for the direct, laser-based synthesis of graphene films on quartz by heating a few layers of

graphene via the heating and decomposition of a photoresist using a continuous wave laser. The graphene film produced from this process is as small as the laser beam itself (diameter of 50 μm). The process, however, requires the preparation of both a substrate and photoresist film. The process cannot be optimized until the fundamental mechanisms underlying the laser-based surface modification are better understood.

In the present study, we developed a simple, one-step, catalyst-free method for forming a transparent conductive region directly on a specific spot of a glass substrate. We investigated three formation mechanisms, namely, deposition of the carbon cluster, the laser-induced diffusion and chemical reaction of the laser-excited carbon clusters, and the formation of graphite structures, using Raman spectroscopy, transmission electron microscopy (TEM), and X-ray photoelectron spectroscopy (XPS).

1. Experimental

Figure 1 shows the experimental setup used in this study. A graphite target (non-HOPG, Nilaco Co., 99.98%, diameter 50 mm) was placed in a stainless steel chamber at a distance of 6.8 mm from a quartz glass substrate (20×20×1 mm, Furuuchi Chemical Co.). The energy was delivered by a pulsed laser (Continuum Inc., Inlite II-50, $\lambda = 532$ nm, 7–9 ns pulse width, 50 Hz repetition rate). The energy delivered per area was adjusted by resizing the laser spot using a concave lens and two convex lenses. The focused laser beam irradiated the target through the quartz substrate in helium gas (267 Pa) at room temperature. The size (and energy density, or fluence) of the laser spot was varied within a range of ϕ1.3 mm (2.3 J cm^{-2}) to ϕ3.3 mm (0.35 J cm^{-2}) by changing the focal distance of the convex lens. The surface of the quartz substrate was exposed to a laser-induced plume during the PLD, and the initial deposits on the substrate were believed to consist of carbon clusters generated by the rapid quenching in the gas phase (Kim *et al.*, 2009). These ablated carbon clusters were deposited on the rear side of the quartz glass, opposite from the laser source. The laser irradiation period was varied in a range from 1 min (3,000 shots) to 20 min (60,000 shots). The electrical conductivity and optical transmission were measured using a four-probe method and spectrophotometer (Ocean Optics) with deuterium and tungsten halogen sources, respectively. The evolution of the carbon structure was analyzed by XPS (AXIS-ULTRA DLD, Shimadzu Corp.) and by micro-Raman spectroscopy (Nanofinder, Tokyo Instruments Inc.) with a 532 nm (0.15 mW) probe laser. The morphology and crystal structure of the final product were assessed by TEM (H-800, Hitachi Ltd.). To prepare TEM specimens, small portions of the film were scraped off using a diamond knife and attached to the TEM grid.

2. Results and Discussion

Figure 2 shows a typical optical image of the surface-modified quartz substrate. This substrate was rotated by motor to substantially expand the area of the surface-modified region (about 8 mm in diameter) in order to better evaluate the optical transparency and sheet resistance. As shown in Figure 2, a transparent spot is clearly observed in the laser-irradiated area (see the center of the picture), while the remaining surface is covered by a black mate-
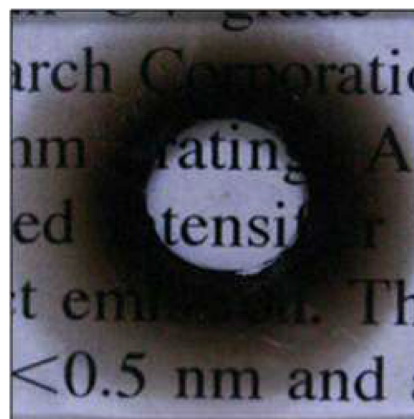

Fig. 2 Example of a carbon-deposited glass substrate (black component) and irradiated area (transparent area)
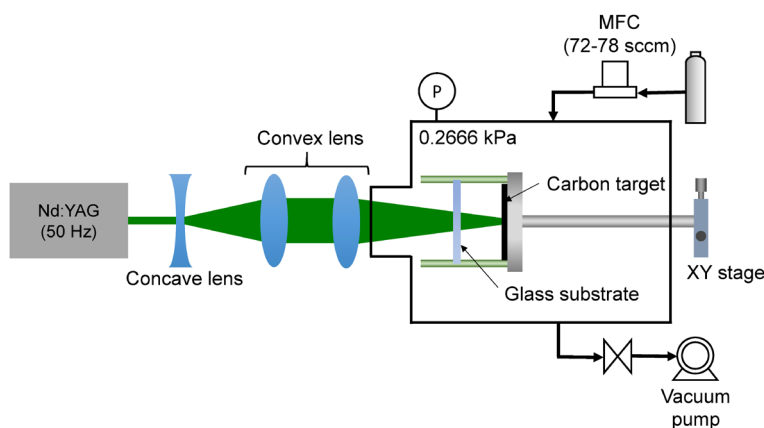

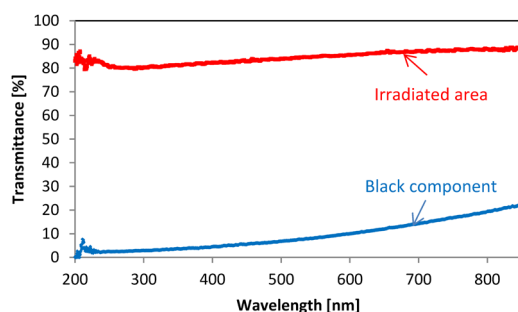**Fig. 1** Experimental setup for surface modification of the quartz glass substrate

Fig. 3 Optical transmittance of the surface-modified quartz substrate at the laser-irradiated spot and black component

rial that was later determined to be amorphous carbon by Raman spectroscopy. **Figure 3** shows the optical transmittance of a typical sample. The light transmittance of the laser-irradiated region exceeded 80% at wavelengths ranging from 200 to 850 nm, while the black component showed a transmittance of less than 30%. The sheet resistance of the laser-irradiated area ranged from 5.5×10^2 to $3.8 \times 10^5 \, \Omega$/sq. and was dependent on both the preparation conditions (to be shown later) and the positions of the probes. This range of values slightly exceeded the sheet resistance of graphene (on the order of $10^2 \, \Omega$/sq.). Note also that extremely high sheet resistance ($>$MΩ/sq) was found in the black area, i.e., the area with deposited carbon clusters. Nevertheless, the successive laser irradiation of carbon clusters created an array of two-dimensional conductive networks (probably sp^2 carbon structures) on the surface of the quartz glass.

The carbon structures of the transparent region can be analyzed in more detail using the representation of the Raman spectra of the transparent region shown in **Figure 4.** The Raman spectroscopy was conducted at the center of a transparent thin film prepared at a fluence of 1 J cm^{-2} at various time intervals during laser irradiation of the substrate without rotation. The figure also shows the surface resistance of the transparent region. The crystal structure of a carbon film can generally be evaluated based on three characteristic Raman peaks corresponding to the G (around 1,580 cm^{-1}), D (1,350 cm^{-1}), and 2D bands (2,700 cm^{-1}) (Tang *et al.*, 2010). The G band is the first order Raman signal from the graphitic hexagonal (sp^2) lattice, while the 2D band is the most important peak representing the formation of the thin layer of graphite structures. The D and D′ peaks that appear at 1,620 cm^{-1} correspond to the disorder and defects in the sp^2 network. As can be seen from Figure 4, the G and 2D bands appear at irradiation times longer than 5 min, indicating the formation of a graphite structure on the quartz surface. The film contained a significant amount of defects (D-band), which may partly explain the higher sheet resistance compared to graphene. After irradiation for 1 min, the deposition of amorphous carbon clusters manifests both as a broad Raman peak and high sheet resistance. The present process, therefore, requires a certain incubation time to trigger the formation of a graphite network on the substrate. The sheet resistance of the laser-irradiated spot
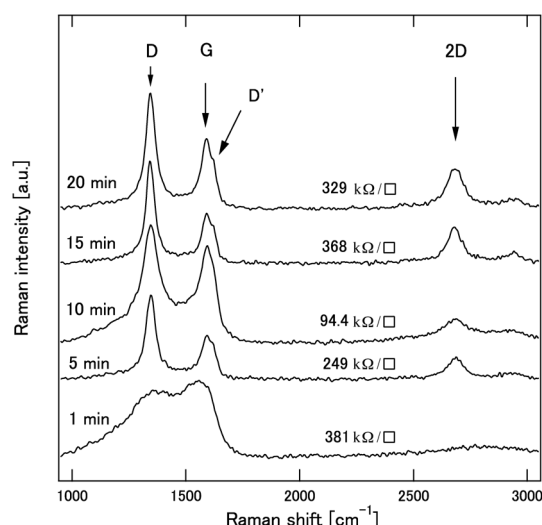

Fig. 4 Raman spectra of the laser-irradiated area at the center at different irradiation durations from 1 to 20 min

was decreased during this incubation time (1 to 10 min), although it decreased again by further ($>$15 min) laser irradiation.

TEM observations and electron diffraction (ED) measurements were conducted to allow for a more detailed analysis of the structures of the laser-irradiated spots. The cross-sectional TEM technique was used to observe graphene on a SiC substrate in an earlier study (Norimatsu and Kusunoki, 2009). We opted against this approach in the present study, however, because cross-sectional TEM specimens can be very difficult to prepare from films on quartz glass. We decided to prepare top-view TEM specimens instead by sequentially cleaving small pieces from the original carbon-deposited quartz surface using a sharp diamond needle. These cleaved pieces were dispersed in ethanol, and the resulting dispersion was dropped onto a micro-grid mounted on a copper mesh for support. The morphology and nanostructure of each specimen were determined using bright-field images (BFIs). The corresponding selected area electron diffraction (SAED) patterns were obtained using a Hitachi H-800 TEM operated at an accelerating voltage of 200 kV. **Figure 5** shows the BFIs and SAED patterns of a sample generated by applying laser irradiation for 15 min at a fluence of 1 J cm^{-2}.

As shown in Figure 5(a), thin flake-like deposits larger than 100 nm were successfully cleaved from the quartz substrate. The inset in Figure 5(a) is an SAED pattern from the thin flake-like deposits. The Debye–Scherrer rings in this pattern can be consistently indexed as those of graphite having a hexagonal structure with lattice constants $a = 2.46$ Å and $c = 6.71$ Å. The lattice spacing of the Debye–Scherrer rings are 3.31, 2.13, and 1.24 Å, which correspond to 0002, 1010, and 1120 lattice planes, respectively. These data indicate that the film shown in Figure 5(a) is graphite, or nanocrystalline graphite. In contrast, Figure 5(b) shows thicker films with more specific areas of contrast. In the SAED pattern inset in Figure 5(b), only halo rings are evident. The
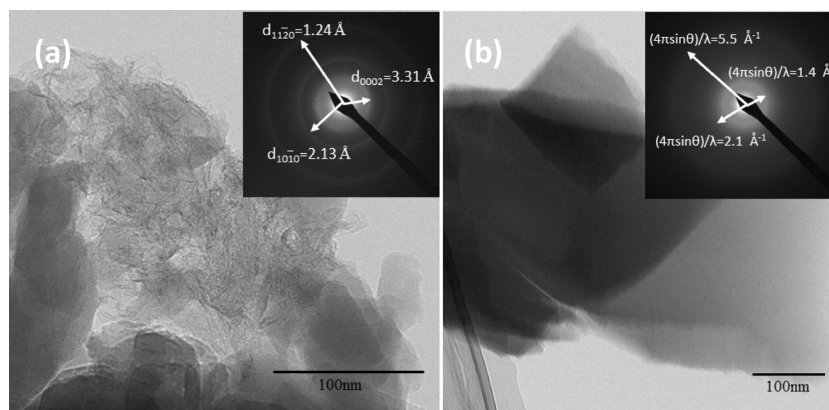
Fig. 5 TEM images and electron diffractions of the fractions of a sample irradiated at $1\,\mathrm{J\,cm^{-2}}$ for 15 min
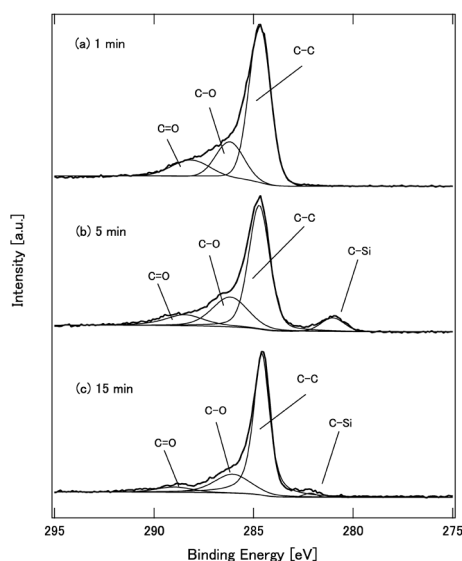

Fig. 6 XPS C1s region of a transparent conductive film generated on a quartz glass substrate by laser irradiation (duration (a) 1 min, (b) 5 min and (c) 15 min)

scattering vector values for the halo rings are approximately 1.4, 2.1 and $5.5\,\text{Å}^{-1}$, corresponding to amorphous SiO_2. This result demonstrates that the thicker films are composed of amorphous SiO_2 fragments cleaved from the substrate. An earlier study by Shimoo *et al.* (1988) confirmed the production of SiC by thermal heating via a reaction between SiO_2 and C. Our TEM observations in the present work yielded no clear evidence of a reaction between SiO_2 and C. To analyze the surface chemistry of the specimens in detail, we decided to carry out a surface chemical analysis using XPS.

Figure 6 shows a typical XPS C1s pattern for the carbon film generated on the quartz glass substrate by laser irradiation for either 1, 5 or 15 min. The quartz substrate was non-conducting, so the XPS peaks tended to shift towards higher binding energies via a surface-charging effect. The spectra in this figure were, therefore, calibrated to set the C1s peak, without a chemical shift, at 284.6 eV. After 1 min of deposition, the C1s spectrum is asymmetric with a tail extending to 290 eV, and can be fitted with three component

peaks centered at approximately 288, 286, and 285 eV (corresponding to C=O, C–O, and C–C, respectively). This result indicates that approximately 30% of the carbon atoms deposited on the substrate were oxidized, possibly due to reactions with silica at the high temperatures caused by the laser irradiation. After 5 min of laser irradiation (Figure 6(b)), a peak due to the C–Si bond clearly appeared at around 281 eV, providing evidence of the formation of SiC on the substrate. The formation of the C–Si bond may play an important role in the formation of the graphite network identified by the Raman spectroscopy after the incubation (>5 min).

Numerous studies on graphene formation from SiC have recently been described. Norimatsu and Kusunoki (2009), for example, observed graphene formation in cross-sectional TEM images of a SiC film surface through the evaporation and desorption of silicon when the SiC was heated to 1,400°C. A similar reaction may have occurred in our study, since the temperature at a substrate surface at $1\,\mathrm{J\,cm^{-2}}$ reaches nearly 6,000°C by ns-pulsed laser irradiation. Lee *et al.* (2010) actually formed a micro-patterned graphene by irradiating a SiC substrate with an excimer laser, but their substrate was limited to non-transparent SiC.

As shown in Figure 6(c), the intensity of the Si–C peak decreased by further (15-min) laser irradiation of the surface. It suggested that the Si–C bond can be seen at the outermost surface only at the incubation time (probably around 5 min). After the formation of Si–C at the outermost surface, it might play a role as a catalyst to grow a graphitic layer and the generated graphitic layer might hide the peak of Si–C in the XPS spectrum. This growth mechanism may be linked with the minimum sheet resistance measured in the 10-min sample (Figure 4). In order to obtain a lower surface resistance film, more precise analyses and control of the growth process may be necessary. However, our process has the advantageous ability to generate micro-scale transparent conductive films, which can be applied for patterning the electrical conductive network directly on the transparent substrates.

Conclusion

Carbon-based transparent conductive films were fabricated directly on quartz glass substrates by the PLD-based process utilizing the light transparency of the substrate. The surface modification of the quartz glass was triggered by the laser-induced formation of a C–Si bond, as confirmed by the XPS. In TEM observation, the thin graphite films were larger than a hundred nanometers in size. Although the electrical conductivity of the surface-modified area should be improved, the proposed synthesis method offers a new technique for the surface modification of a small area of quartz glass by a simple one-step method.

Acknowledgements

Literature Cited

Bonaccorso, F., Z. Sun, T. Hasan and A. C. Ferrari; "Graphene Photonics and Optoelectronics," *Nat. Photonics*, **4**, 611–622 (2010)

Chhajed, S., F. S. Martin, J. K. Kim and E. F. Schubert; "Nanostructured Multilayer Graded-Index Antireflection Coating for Si Solar Cells with Broadband and Omnidirectional Characteristics," *Appl. Phys. Lett.*, **93**, 251108 (2008)

Geim, A. K. and K. S. Novoselov; "The Rise of Graphene," *Nat. Mater.*, **6**, 183–191 (2007)

Geim, A. K.; "Graphene: Status and Prospects," *Science*, **324**, 1530–1534 (2009)

Granqvist, C. G. and A. Hultaker; "Transparent and Conducting ITO Films: New Developments and Applications," *Thin Solid Films*, **411**, 1–5 (2002)

Kim, K. S., Y. Zhao, H. Jang, S. Y. Lee, J. M. Kim, K. S. Kim, J. H. Ahn, P. Kim, J. Choi and B. H. Hong; "Large-Scale Pattern Growth of Graphene Films for Stretchable Transparent Electrodes," *Nature*, **457**, 706–710 (2009)

Krishnamurthy, V. and I. L. Kamel; "Argon Plasma Treatment of Glass Surfaces," *J. Mater. Sci.*, **24**, 3345–3352 (1989)

Lee, D., M. F. Toney, W. Ko, J. C. Randel, H. J. Jung, K. Munakata, J. Lu, T. H. Geballe, M. R. Beasley, R. Sinclair, H. C. Manoharan and A. Salleo; "Laser-Synthesized Epitaxial Graphene," *ACS Nano*, **4**, 7524–7530 (2010)

Li, X., W. Cai, J. An, S. Kim, J. Nah, D. Yang, R. Piner, A. Velamakanni, I. Jung, E. Tutuc, S. K. Banerjee, L. Colombo and E. S. Ruoff; "Large-Area Synthesis of High-Quality and Uniform Graphene Films on Copper Foils," *Science*, **324**, 1312–1314 (2009)

Matthews, M. J., S. T. Yang, N. Shen, S. Elhadj, R. N. Raman, L. L. Guss, I. L. Bass, C. N. Michael and P. J. Wegner; "Micro-Shaping, Polishing, and Damage Repair of Fused Silica Surfaces Using Focused Infrared Laser Beams," *Adv. Eng. Mater.*, **17**, 247–252 (2015)

Norimatsu, W. and M. Kusunoki; "Transitional Structures of the Interface between Graphene and 6H–SiC (0 0 0 1)," *Chem. Phys. Lett.*, **468**, 52–56 (2009)

Qian, M., Y. S. Zhou, Y. Gao, J. B. Park, T. Feng, S. M. Huang, Z. Sun, L. Jiang and Y. F. Lu; "Formation of Graphene Sheets through Laser Exfoliation of Highly Ordered Pyrolytic Graphite," *Appl. Phys. Lett.*, **98**, 173108 (2011)

Shimoo, T., F. Mizutaki, S. Ando and H. Kimura; "Mechanism of Formation of SiC by Reaction of SiO with Graphite and CO," *J. Japan Inst. Metals*, **52**, 279–287 (1988)

Tang, B., H. Guoxin and H. Y. Gao; "Raman Spectroscopic Characterization of Graphene," *Appl. Spectrosc. Rev.*, **45**, 369–407 (2010)

Wang, K., G. Tai, K. H. Wong, S. P. Lau and W. Guo; "Ni Induced Few-Layer Graphene Growth at Low Temperature by Pulsed Laser Deposition," *AIP Advanced*, **1**, 022141 (2011)

Wei, D., J. I. Mitchell, C. Tansarawiput, W. Nam, M. Qi, P. D. Ye and X. Xu; "Laser Direct Synthesis of Graphene on Quartz," *Carbon*, **53**, 374–379 (2013)

Zheng, M., K. Takei, B. Hsia, H. Fang, X. Zhang, N. Ferralis, H. Ko, Y. L. Chueh, Y. G. Zhang, R. Maboudian and A. Javey; "Metal–Catalyzed Crystallization of Amorphous Carbon to Graphene," *Appl. Phys. Lett.*, **96**, 063110 (2010)